공학석사 학위논문

Efficient Intratumoral Delivery of Oncolytic Vaccinia Virus Using Keratin-based Hydrogel into Breast Cancer

항암 백시니아 바이러스의 국소적 전달을 위한
케라틴 기반 하이드로젤 연구

2018년 2월

서울대학교 대학원

협동과정 바이오엔지니어링 전공

윤 연 희

Efficient Intratumoral Delivery of Oncolytic Vaccinia Virus Using Keratin-based Hydrogel into Breast Cancer

항암 백시니아 바이러스의 국소적 전달을 위한
케라틴 기반 하이드로젤 연구

지도 교수 김 병 수

이 논문을 공학석사 학위논문으로 제출함

2018년 2월

서울대학교 대학원
협동과정 바이오엔지니어링전공
윤 연 희

윤연희의 석사 학위논문을 인준함
2018년 2월

위 원 장 황 석 연 (인)
부 위 원 장 김 병 수 (인)
위 원 백 승 렬 (인)

Abstract

Efficient Intratumoral Delivery of Oncolytic Vaccinia Virus Using Keratin-based Hydrogel into Breast Cancer

Yun Hee Youn
Interdisciplinary Program for Bioengineering
The Graduate School
Seoul National University

Basal-like breast cancers have been found to be highly malignant, which cannot be treated with a hormonal therapy, as they lack expression of estrogen-receptor, progesterone receptor, and human epidermal growth factor receptor type 2. The introduction of gene therapy has paved the way to combat those basal-like breast cancers or triple-negative breast cancer. Oncolytic vaccinia virus has been genetically engineered for targeted anti-cancer therapy against various types of tumor through gene-mediated mechanisms as cancer cell-selective replication and cell lysis. However, the clinical efficacy of oncolytic virus has been limited for complete remission of cancer due to complex immunological reaction of the human body, high dose-dependency of oncolytic virus, and difficult distribution throughout the dense tumor cells. For these reasons, we developed an oncolytic virus delivery system using keratin-crosslinked hyaluronic acid hydrogels for both

sustained release of virus in the tumor tissue and synergetic anti-tumoral effect of human hair-extracted keratin. This injectable hydrogel delivery system would improve subcutaneously localization and protection of virus from antiviral environment in breast tumor tissue. T cells and cytokine levels were also upregulated by viral delivery with injectable hydrogel. Furthermore, histological examination revealed that necrotic tumor lesion was increased by intratumoral virotherapy in mouse 4T1 cell carcinoma syngeneic model. The results suggest that the viral delivery with biocompatible injectable hydrogel provided an improved tumor targeting and antitumor efficiency of virotherapy for treatment of cancer.

Keywords: Oncolytic virus, Cancer virotherapy, Injectable hydrogel, Intratumoral delivery, Drug delivery system

Student Number: 2016-21174

Table of Contents

List of Figures

Figure 7. Evaluation of apoptosis imaging by Annexin V/PI staining of KTN-based hydrogels with OVV (MOI 1) in 4T1 mouse breast cancer cell line (Scale bar = 200 μm)

Figure 8. *In vivo* fluorescence images of Cy5.5-labeled KTN-HHA in tumor-bearing BALB/c mouse and stably remained for 14 days (Scale bar = 200 μm)

Figure 9. *In vivo* tumor volume growth curve of after treatment of OVV loaded KTN-based hydrogels in tumor-bearing BALB/c mouse for 19 days

Figure 10. The gross tumor morphology (a) and the terminal tumor weight (b) of 4T1 mouse breast cancer cells bearing mice after intratumoral injection of OVV loaded KTN-based hydrogels

Figure 11. Histological section of tumor of 4T1 cell bearing mice with H&E staining (Scale bar = 2 mm) (a), tumor area analysis excluding tumor necrosis (b), and metastatic region of 4T1 cells on the lung of the mice (c)

Figure 12. Immunohistochemical staining of OVV, CD4 positive cell, and CD8 positive cell infiltration

Figure 13. Flow cytometry analysis of immune cell distribution

1. Introduction

Unlike previously identified subtypes of breast cancers, triple-negative breast cancer (TNBC) has been recently researched as it lacks specific receptors such as estrogen receptor (ER), progesterone receptor (PR), and human epidermal growth factor receptor type 2 (HER2) [1-3]. The heterogeneity of TNBCs at the genetic level makes it difficult to completely cure localized tumors as well as metastatic cancers [1]. Thus, apart from the active targeting of hormonal therapy, other treatments are required to treat TNBCs.

Viral vector for cancer therapy has been actively researched in biomedical engineering for a decade recently [4, 5]. One of the viral vectors named oncolytic vaccinia virus (OVV) is genetically programmed to replicate within cancer cells and directly induce cell lysis or apoptosis [6, 7]. The OVVs kill cancer cells as they take over the cellular translational and transcriptional machinery, ultimately leading to an induction of cell necrosis or apoptosis. Original vaccinia encodes a thymidine kinase (TK) gene that, when deleted, leads to dependence of the virus on cellular TK expression [8]. Cellular TK, which is regulated by the E2f transcription factors, is transiently expressed during the S phase of the cell cycle in proliferating normal cells, but is constitutively expressed at high levels in the majority of cancers regardless of proliferation status [9]. Vaccinia also expresses vaccinia growth factor (VGF), which is secreted from infected cells, inducing proliferation in both infected and surrounding non-infected cells [8]. Therefore, vaccinia strains with deletions in both TK and VGF show selective replication in cancers (Figure 1).

Currently available clinical OVVs have been used as promising agent for cancer virotherapy. Also, it may allow TNBCs to be treated both intravenously and intratumorally without complicated hormonal therapy or cytotoxic chemotherapies.

However, the naked OVV is inefficient to be evenly distributed throughout the tumor tissue that is packed with extracellular matrix of cancer cells [10, 11]. In addition, viral proliferation may be limited because of immune clearance in the tumor tissues [12]. Therefore, efficient delivery of OVVs using locally injectable hydrogels is expected to enhance distribution ability of oncolytic viruses throughout the tumor mass with low doses rather than high, even with enhanced stability of viruses in the body fluid. In this study, we developed keratin-crosslinked hyaluronic acid hydrogel as an OVV delivery system directly injected into a tumor tissue.

Extracted keratin (KTN) from human hair has been reported to have the ability of apoptosis on cancer cells by Markowicz et al. [13]. To enhance hydrophilicity and high-water content capacity, KTN proteins were synthesized with natural hydrophilic polymer, hyaluronic acid (HA) [14]. The KTN-crosslinked HA allows the hydrogels to be injectable and provides the hydrophilic interaction with OVVs.

HA hydrogels are widely pursued as drug delivery materials due to their excellent biocompatibility and biodegradability [15]. HA has been chemically modified and crosslinked to produce three dimensional hydrogel structures that swell in aqueous environments [16].

Here, we report the *in vitro* characterization of OVV entrapped in KTN-based hydrogels, prolonged gene expression as a result of the sustained OVV

release and protective microenvironment within the gel, and enhanced OVV-mediated cancer cell killing. We also demonstrated that local injection of labeled KTN-based hydrogel with long-term localization in the tumor tissue *in vivo*. Enhanced local preferential replication of OVVs mediated by sustained release in the protective gel was determined by immunohistochemical analysis.

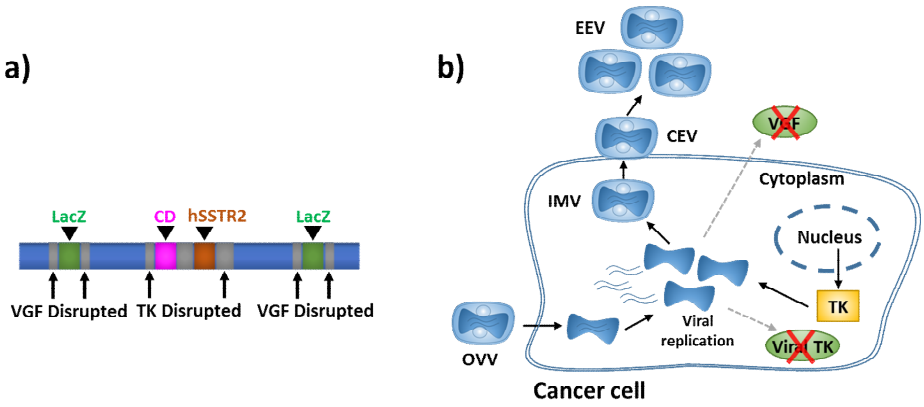

Figure 1. Schematic diagram of recombinant oncolytic vaccinia genomes with primary positions indicated (a) and its mechanism of OVV (oncolytic vaccinia virus) infecting a cancer cell (b)

2. Experimental Section

2.1 Materials

The human hair samples were obtained by healthy donors with no chemically modified and natural black colored hair. Sodium hyaluronate, the sodium salt of hyaluronic acid (HA), with a molecular weight of 50 kDa was purchased from Lifecore Biomedical, LLC, USA. HA with a molecular weight of 2,500 kDa was obtained by Genoss, Korea. Urea, thiourea, 2-mercaptoethanol, Trizma® base, hydrochloric acid (HCl) and Annexin V staining kit were purchased from Sigma-Aldrich, St. Louis, MO, USA. Peracetic acid was purchased by Dongmyung ONC, Korea. Vacuum-driven filtration system were purchased from Merk milipore. Pre-treated RCtubing (MWCO: 12-14 kDa) was purchased from Spectrum Laboratories, Inc., USA. Genetically engineered oncolytic vaccinia virus (JX-929) was kindly provided from SillaJen Inc., Busan, Korea. QIAamp® MinElute virus spin kit was purchased from Qiagen, Germany. For cell culture, RPMI-1640, trypsin-EDTA, fetal bovine serum (FBS), penicillin-streptomycin (PS) and Dulbecco's phosphate-buffered saline (DPBS) were purchased from GIBCO BRL, Invitrogen Co., USA.

2.2 Extraction of Keratin from Human Hair

Keratin (KTN) was extracted from human hair as described previously [17, 18]. Briefly, 20 g of 15 cm long human hair samples were washed with light detergent and rinsed with distilled water several times. For delipidization, the samples were soaked in the solution containing chloroform and methanol (2 : 1 v/v) for 24 hours and washed with distilled water until the remains were completely removed. The human hair samples were air-dried. Dried human hair samples were soaked into the 2% peracetic acid solution for 12 hours at 37 ℃. 400 mL of Shindai solution containing 5% mercaptoethanol, 5 M urea, 2.6 M thiourea and 25 mM Trizma® base (pH8.5) was used for 20 g of human hair samples. After centrifugation, supernatant of the KTN solution was dialyzed using a cellulose membrane (MWCO: 12-14 kDa) against distilled water. The dialyzed KTN is made into a powder state by freeze drying. After the solution was lyophilized, it was stored at –80 ℃.

2.3 Synthesis of Keratin-Crosslinked with Hyaluronic Acid

Crosslinking of KTN to HA was performed by click reaction [16]. 400 mg of 50 kDa HA powders were perfectly dissolved in 80 mL of distilled water. 10 mL of 5 mM 4-(4,6-Dimethoxy-1,3,5-triazin-2-yl)-4-methylmorpholinium Chloride (DMTMM) solution was added into the HA solution. Finally, 400 mg of KTN dissolved in distilled water was added into the mixture and stirred at room temperature for 72 h. For synthesis of 2500 kDa HA and KTN, 160 mg of HA were dissolved in 100 mL of distilled water. 10 mL of 5 mL DMTMM solution and 640 mg of KTN dissolved in distilled water were added, in the same manner as in the synthesis of low molecular weight HA.

Both solutions are synthesized using a stirrer for 3 days. The resulting solutions were dialyzed against distilled water for 5 days using a 10 kDa cutoff spectra/Pro dialysis membrane (Spectrum). The dialyzed KTN-HA solutions are lyophilized by freeze-drying and stored at –80 ℃.

2.4 Characterization of Keratin and Keratin-based Hydrogel

The molecular weight of the extracted KTN was measured by sodium dodecyl sulfate poly-acrylamide gel electrophoresis (SDS-PAGE). KTN samples (1% and 2% w/v) were reduced using the 2X SDS-PAGE loading buffer (Biosesang, Korea) by heating 95 ℃ for 5 min and run in a 12% Bio-Tris gel at 200 V for approximately 30 minutes. Lugen^{TM} Sensi Plus Prestained Protein Markers Broad Range (5 – 245 kDa) was used as the protein marker. ^{1}H-NMR spectra were recorded in deurerium oxide (D_2O) on a Bruker Avance, 400 MHz instrument. 5 mg of KTN powder, 50 kDa and 2500 kDa HA, KTN-low molecular weight HA (KTN-LHA) and KTN-high molecular weight HA (KTN-HHA) were dissolved in 1 mL of D_2O. All reactions were monitored using ^{1}H-NMR (Bruker Avance, 400 MHz). Viscosity was measured for comparison of physical viscosities of KTN-HA hydrogels synthesized from HA of two different molecular weight. After dissolving 2% (w/v) KTN-LHA and 1.25% (w/v) KTN-HHA in distilled water and transferring 1 mL each to a 40 mm parallel plate, a rotational rheometer Bohlin Gemini (Malvern Instruments) was used. The temperature of suspensions during experiments was maintained at 25 ℃. Viscosity measurements were carried out in triplicate. The surface morphologies of the KTN, KTN-LHA and KTN-HHA were characterized using a scanning electron microscope (SEM). SEM (S-4700, Hitachi, Japan) measurements were carried out after the samples were preconditioned by using a Pt sputter-coating system (Eiko IB3, Tokyo, Japan).

2.5 Cell Culture

NIH/3T3 (Mouse fibroblast cell line) was cultured in DMEM supplemented with 10% (v/v) of FBS (Fetal bovine serum) and 1% (v/v) of PS (Penicillin streptomycin solution). 4T1 (Mouse breast cancer cell line) and MCF-7 (Human breast cancer cell line) were cultured in RPMI 1640 supplemented with 10% (v/v) of FBS (Fetal bovine serum), 1% (v/v) of PS (Penicillin streptomycyn solution) and 10 mM HEPES. The cells were incubated under humidified 5% CO^2 atmosphere at 37 ℃.

2.6 *In Vitro* Hydrogel Cytotoxicity Test

The cytotoxicity of synthesized hydrogels on normal cells of NIH/3T3 was evaluated with Cell counting kit-8 (CCK-8) assay. 2×10^3 cells/100 μL of NIH/3T3 cells were seeded to a well in 96-well plate and stabilized for 24 hours. Then, 20 μL of 1% (w/v) KTN, 2% KTN-LHA and 1.25% KTN-HHA are dropped on the cells and filled with 180 μL of cell growth medium (DMEM). After incubation for 24 hours and 48 hours, the dishes of time point were washed with DPBS (pH 7.4) to remove dead cells and), and cell viability was measured by CCK-8 assay. The experimental groups were compared with the control DPBS group.

2.7 *In Vitro* Release Study of Virus from Hydrogel

For the encapsulation of vaccinia virus within the KTN-based hydrogels, vaccinia virus (1×10^7 pfu) was mixed into KTN, KTN-LHA, and KTN-HHA at the same concentrations as in the above cytotoxicity experiment of 50 μL. In a 24-well plate, the hydrogels were placed on a 3-μm pore size hanging insert and the released viruses were quantified in 1 mL DPBS. After shaking incubation for 30 minutes, 2, 6, 24, 48, 96, and 168 hours from the start of release, the virus released from the gel was obtained from 1 mL DPBS. The viral DNA was extracted using QIAamp MinElute Virus Spin Kit (Qiagen). For the real-time Q-PCR analysis, the extracted DNA samples were quantified using SYBR Green (Invitrogen). Real-time Q-PCR was performed by using ABI Prism 7500 (Applied Biosystems). Target genes and their primers were as follows: 5'-GAA CAT TTT TGG CAG AGA GAG CC-3' (target genes), 5'-GAA CAT TTT TGG CAG AGA GAG CC-3' (forward) and 5'-CAA CTC TTA GCC GAA GCG TAT GAG-3' (reverse) in the E9L region of vaccinia virus.

2.8 *In Vitro* Cancer Cell Viability of Virus-loaded Hydrogel

To evaluate the anti-cancer activity of KTN-based hydrogels, 4T1 mouse breast cancer cell line and MCF-7 human breast cancer cell line were dispensed in a 96-well plate at 2×10^3 cells/100 μL. After stabilization for 24 hours, the cells were treated by 20 μL dropwise of KTN-based hydrogels containing different concentration of viruses. The experimental groups are KTN, KTN-LHA and KTN-HHA containing OVVs from 0 to 1 in the range of multiplicity of infection (MOI). After the medium is filled with 180 μL, cell activity is evaluated by CCK-8 assay 48 hours later. In the CCK-8 assay, 10% CCK-8 solution is diluted in DMEM without FBS and treated with 100 μL per well. After incubation for 2 hours at 37 ℃ incubation, the ratio is calculated by comparison with any untreated cells after measurement at 450 nm with a Benchmark Plus™ microplate spectrophotometer (BIO-RAD). The cytotoxicity was evaluated with Cell counting kit-8 (CCK-8) assay.

2.9 *In Vitro* Cancer Cell Imaging of Virus-loaded Hydrogel

To evaluate the anti-carcinogenic activity of KTN-HA entrapped OVVs, the mouse breast cancer cell line 4T1 was dispensed at a density of 2×10^3 cells/100 μL into a 96-well plate. After stabilization for 24 hours, the cells were treated with 20 μL dropwise of KTN, KTN-LHA and KTN-HHA from 0 to 1 in the range of MOI of OVVs. After the medium was filled with 180 μL onto each well, the Live & Dead assay was evaluated 48 hours later. Calcein AM is a principle that stains cytoplasm of living cells to green fluorescence and stains the nuclei of dead cells with EthD-1. 0.5 μL of 4 mM calcein solution and 1 μL of 2 mM EthD-1 solution are diluted in 1 mL of DPBS, treated with 60 μL of each sample, incubated for 5 minutes, and observed with a fluorescence microscope.

Annexin V-FITC Apoptosis Detection kit (Sigma Aldrich) was used to measure cell necrosis of breast cancer cells by imaging. Annexin V stains the cell membrane at the early stage of apoptosis with green fluorescence, while propium iodine (PI) intercalates into the DNA of necrotic cells and displays red fluorescence imaging. Finally, the nuclei of all cells were stained with 4', 6-diamidino-2-phenylindole (DAPI) staining, and stained with blue for 3 minutes and observed with a fluorescence microscope.

2.10 *In Vivo* Hydrogel Imaging in Tumor-bearing Mouse

Fluorescence Cyanine-5.5 (Cy5.5) was conjugated to confirm the extent of KTN-HA residing in cancer tissues and confirmed by imaging. To monitor *in vivo* biodistribution of KTN-HHA-Cy5.5, 6-week-old female Balb/c mice were prepared (each group n=3). The mice were subcutaneously inoculated with 4T1 (5×10^5 cells per a mouse) into the 4^{th} right mammary fat pad of the mice. 50 μL of KTN-HHA-Cy5.5 solution was injected intratumorally into the tumor-bearing mice. After injection, the biodistribution of tumor in mice was monitored by using the Xenogen IVIS 200 Imaging System (PerkinElmer, UK) over a 14-day period after intratumoral injection.

2.11 *In Vivo* Evaluation of Tumor Inhibition Effect

The experimental procedures were performed in compliance with protocols approved by the Institutional Animal Care and Use Committee of Konkuk University (KU17066). To establish orthotopic 4T1 model, 5×10^5 4T1 tumor cells mixed with matrigel (1:1, v/v) were injected into 4th mammary fat pad of female 6-week-old BALB/c. Tumor sizes were measured using calipers and the treatment began when the tumor sizes reached 60~80 mm^3. Mice were randomly allocated into four groups (n = 6 per group) as follows: a Con group with DPBS (50 μL) injection; a Virus group with OVV (1×107 pfu/50 μL) injection; a KTN group with 1% (w/v) of KTN solution (50 μL) injection; a KTN-HHA group with 1.25% of KTN-HHA solution (50 μL) injection; a KTN+V group with OVV (1×107 pfu/50 μL) loaded KTN solution injection; a KTN-HHA+V group with OVV (1×107 pfu/50 μL) loaded KTN-HHA hydrogel injection. All treatments were given intratumorally 3 times repeatedly at intervals of 5 days. Mice were euthanized at 19 days post-treatment on the first injection, tumor tissues along with vital organs were collected for histological analysis and peripheral blood was collected for flow cytometric analysis.

2.12 Histological Evaluation

The tumor tissues and vital organs including lung, heart, liver, kidney and spleen were harvested, fixed with 10% neutered buffed formalin (BBC Biochemical, WA, USA). The tissues were embedded in paraffin and sections (4 μm in thickness) were stained using hematoxylin and eosin (H&E) for histological analysis. For immunohistochemistry, sections were stained by standard method using mouse anti-CD8 (Santa Cruz Biotechnology), rabbit anti-CD4 (Santa Cruz Biotechnology), and rabbit anti-vaccinia virus (Abcam). Then the sections were either incubated with Vectastain® Elite ABC-Peroxidase kit (Vector Laboratories, CA, USA), visualized by Vector SG (Vector Laboratories) and counterstained with nuclear fast solutions (Vector Laboratories).

2.13 Flow Cytometry of Immune Cell Distribution

Peripheral blood samples were collected and red blood cells were lysed with RBC lysis buffer. Cells were washed in PBS containing 1% FBS, then stained with monoclonal mouse anti-CD8 (Santa Cruz Biotechnology, CA, USA), rabbit anti-CD4 (Santa Cruz Biotechnology), rabbit anti-CD3 (Abcam, Cambridge, UK), mouse anti-CD25 (Thermo Fisher Scientific, MA, USA), rat anti-Gr1 (Thermo Fisher Scientific), rabbit anti-CD11b (Santa Cruz Biotechnology), rat anti-Nkp46 (Biolegend, CA, UAS), mouse anti-Nk1.1 (Thermo Fisher Scientific), mouse anti-CD56 (Abcam) antibodies. Cells were fixed with 4% paraformaldehyde then incubated with FITC or Alexa fluor-conjugated antibodies (Santa Cruz Biotechnology). For each sample, 10,000 cells were analyzed using FACS Calibur instrument (BD biosciences, CA, USA).

2.14 Statistical Analysis

All values are depicted as mean ± standard deviation (SD). Statistical analysis was carried out in GraphPad Prism 5.0 (GraphPad Software, San Diego, CA). All statistical analyses were performed using unpaired two-tailed Student's t-tests (two groups) and one-way ANOVA with Tukey's post-hoc tests (for more than two groups). Pairs with p-values (*, $^{\#}$, $^{\dagger}P < 0.05$; **, $^{\#\#}$, $^{\dagger\dagger}P < 0.01$) were considered statistically significant.

3. Results and Discussion

3.1 Development and Characterization of Keratin-based Hydrogel

For enhancing antitumoral efficiency of OVV, in the present study, we designed the KTN-crosslinked HA by click reaction (Figure 2a). The KTN shows the anticancer effect as studied before [13] and the HA backbone can retain water, which may reserve hydrophilic OVV in the synthesized KTN-HA hydrogel.

To observe the molecular weight of extracted KTN from human hair, we performed 2X SDS-PAGE of 1% and 2% (w/v) of KTN (Figure 2b). When KTN was added to each lane, the band appeared at 45 – 65 kDa. This confirms the KTN extraction by the molecular weight characteristics of α-keratin [19].

The synthesis of KTN-HA hydrogel was confirmed by ^{1}H-NMR (Figure 2c). The hydrogel was synthesized by crosslinking the amine group of the KTN protein and the carboxyl group of the hydrophilic polymer HA with DMTMM. The ^{1}H-NMR peaks of low-molecular HA and high molecular HA were measured, and KTN synthesized with HA having different molecular weights was also measured and compared separately. The peaks of KTN and HA were observed in synthesized KTN – HA peaks, confirming that the synthesis was successful.

We identified the rheological properties of each KTN-based hydrogel sample by oscillatory shear measurements with the aim of optimizing the composition of

gel for intratumoral injection. The viscosity (Pas) was measured for comparison of the physical viscosities of KTN-HA hydrogels synthesized from HA of different molecular weight (Figure 2d). When comparing the viscosity of 2% (w/v) KTN-LHA with 1.25% (w/v) KTN-HHA, these rheological properties were not significantly influenced by crosslinking density as well as concentration of the hydrogel. Therefore, we expect to see the cell reaction by the molecular weight of HA completely without the physical difference of the two hydrogels. It proved that HA can provide viscosity in the presence of water as aqueous solutions by their innate capacity to absorb large volumes of water.

To analyze the morphological changes of the synthesized KTN-based hydrogels, we performed SEM analysis. In figure 3, the ×10.0k magnified images of KTN, KTN-LHA, and KTN-HHA are obtained. While KTN shows a fragment of several short strands, both KTN-LHA and KTN-HHA form pores as crosslinked with DMTMM. Compared to KTN-LHA, KTN-HHA has a smaller pore size and denser and smoother surface.

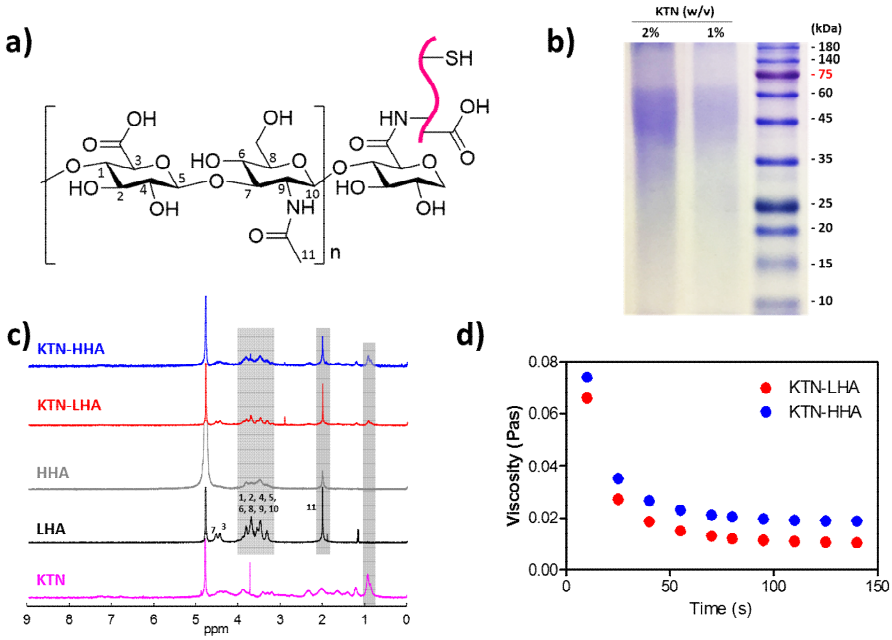

Figure 2. Chemical structure and proton numbering of KTN-HA (a), SDS-PAGE of extracted KTN (b), ^{1}H-NMR (c), and viscosity (d) of KTN-HA

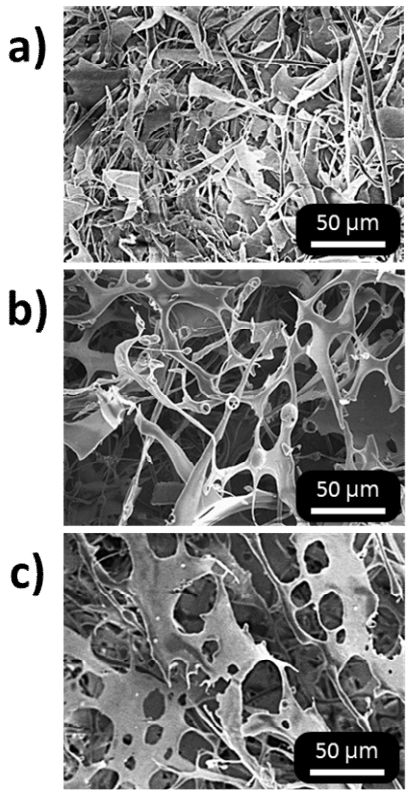

Figure 3. SEM images of KTN (a), KTN-LHA (b), and KTN-HHA (c)

3.2 *In Vitro* Keratin-based Hydrogel Cytotoxicity

In order to test the biocompatibility of KTN and the synthesized KTN-HA, we carried out cell viability test of KTN, KTN-LHA, KTN-HHA. Cell activity of normal fibroblast cell line (NIH/3T3) was measured (Figure 4a) at 24, 48 hours after DPBS, KTN, KTN-LHA, and KTN-HHA were treated. Through the analysis of rheological properties (Figure 2d), 2% (w/v) of KTN-LHA and 1.25% (w/v) of KTN-HHA were confirmed that they have the similar physical properties. Both concentrations of KTN-LHA and KTN-HHA have 1% (w/v) of KTN as the synthesis ratio of each polymer. Thus, the concentration of KTN for cytotoxicity test was set at 1% (w/v). Cell viability results were normalized to the relative percentages of the absorbance of DPBS control group after 24 h of incubation. All showed 48 hours to 2 times more cell activity than 24 hours, indicating no toxicity to normal cells.

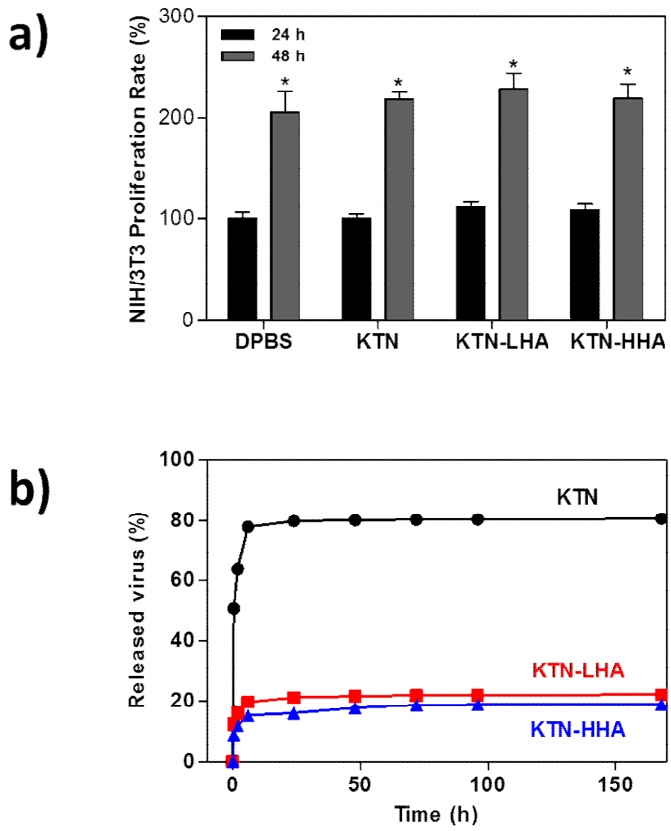

Figure 4. Normal cell as mouse fibroblasts of NIH/3T3 viability after treatment of KTN-based hydrogels (a) and the release test of OVVs released from OVVs loaded into the KTN-based hydrogels for 7 days (b) (*; Compared to 24 h on each group)

3.3 *In Vitro* Quantification of Released Virus from Hydrogel

Real-time qPCR was performed to assess the ability of the KTN-HA loaded with OVV to release OVV (Figure 4b). 1×10^7 pfu of OVV was loaded on KTN, KTN-LHA, and KTN-HHA, and the release performance was evaluated for 7 days. In the KTN, the release rate of the OVV was found to be 50.7% in the first 30 minutes, followed by 12.4% in KTN-LHA and 9% in KTN-HHA. This can be related to the morphological characteristics of the hydrogel. As can be seen from the SEM image, pore was formed in the KTN crosslinked low molecular weight HA rather than KTN, and the pore size of the KTN-HA hydrogel in which the high molecular weight HA was densely crosslinked rather than the low molecular HA (Figure 3) [17]. Therefore, if the OVV is carried in a pore, the OVV can be expected to be slowly released.

3.4 *In Vitro* Anticancer Effect of Virus-loaded Hydrogel

To evaluate the anticancer activity by sustained release effect of OVV from KTN-based hydrogels, 4T1 (Figure 5a) mouse breast cancer cell line and MCF-7 (Figure 5b) human breast cancer cell line were used to with the OVV concentration MOI 0 to 1 loaded in KTN, KTN-LHA, and KTN-HHA. When cell activity was measured after incubation at 37 ℃ for 48 hours, the cell death rate was found to be higher in KTN, KTN-LHA, and KTN-HHA-loaded OVVs than in the case of only OVV (MOI 0, DPBS). In addition, the higher the MOI, the higher the cancer cell death rate was found in both cell lines. In the comparison between KTN-LHA and KTN-HHA, they exhibit different cellular responses according to MOI but do not show a significant difference except for MOI 1 on MCF7.

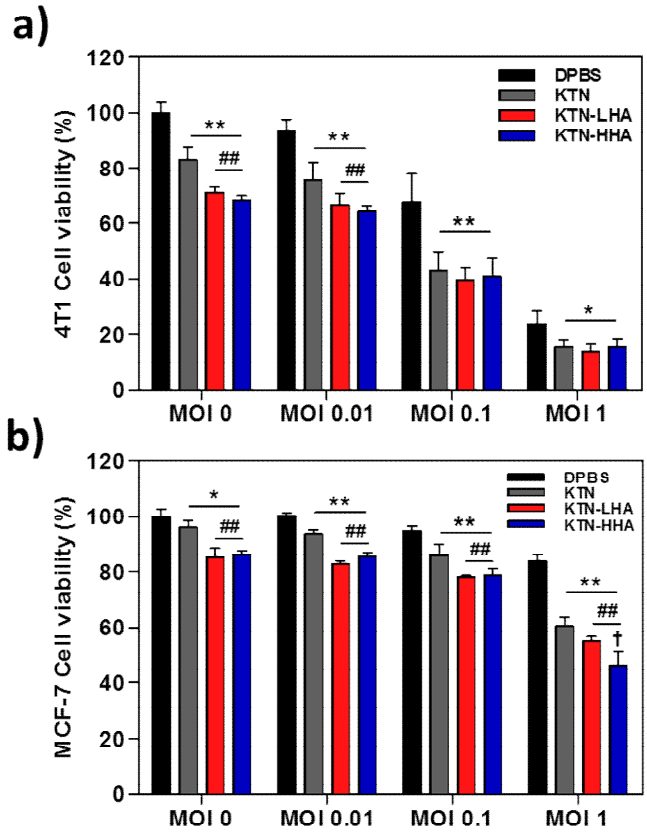

Figure 5. Anticancer effect evaluation of KTN-based hydrogels on 4T1 mouse breast cancer cell line (a) and MCF7 human breast cancer cell line (b) with different concentration of OVV loaded (*; Compared to DPBS, #; Compared to KTN, †; Compared to KTN-LHA)

3.5 *In Vitro* Cancer Cell Imaging for Anticancer Effect

In order to visually observe the anticancer activity of KTN-HA in the breast cancer cell line 4T1, it was treated with the KTN, KTN-LHA, and KTN-HHA, respectively, ranging from 0 to 1 in the range of MOI of OVVs. Cells were treated for 48 h and evaluated for Live & Dead assay (Figure 6). Calcein AM is a principle that stains cytoplasm of living cells to green fluorescence and EthD-1 stains the nuclei of dead cells to red image [20]. As the MOI increased, the highest cell death rate could be confirmed by imaging of KTN-HHA treated cells. Cells that have already died and die are washed away most of the time after dyeing, showing a lot of empty cells.

To determine cell necrosis in breast cancer cell lines using imaging, Annexin V-FITC Apoptosis Detection kit was used (Figure 7). Annexin V is expressed in association with phospholipids such as phophatydylserine, which is exposed inside the cell due to the membrane structure being destroyed at the initial stage when the cell suicides. Therefore, Annexin V stains the cell membrane at the early stage of apoptosis with green fluorescence, and PI also interferes with the DNA of the necrotic cells and displays red fluorescence imaging [21, 22]. Finally, the nuclei of all cells are stained with blue through DAPI staining to confirm the amount of cells. In the DPBS-treated cells, almost no cytotoxicity was observed, and higher cell necrosis was observed in the KTN, KTN-LHA, and KTN-HHA-loaded virus groups than in the group treated with only the OVV of MOI 1 and confirmed by

staining. These results were similar to those of the cell viability assay. The visualization found that the number of living cells and viability were slightly decreased as MOI of OVV increased and KTN-based hydrogels treated.

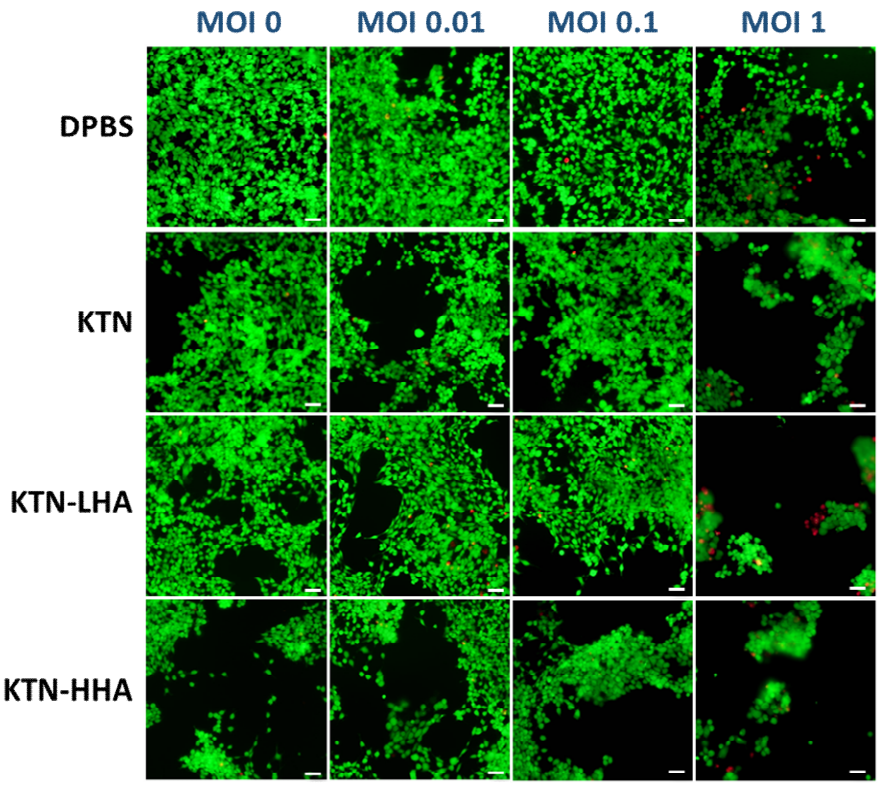

Figure 6. Live & Dead assay imaging of KTN-base hydrogels with OVV (MOI 0 – 1) in 4T1 mouse breast cancer cell (Scale bar = 200 μm)

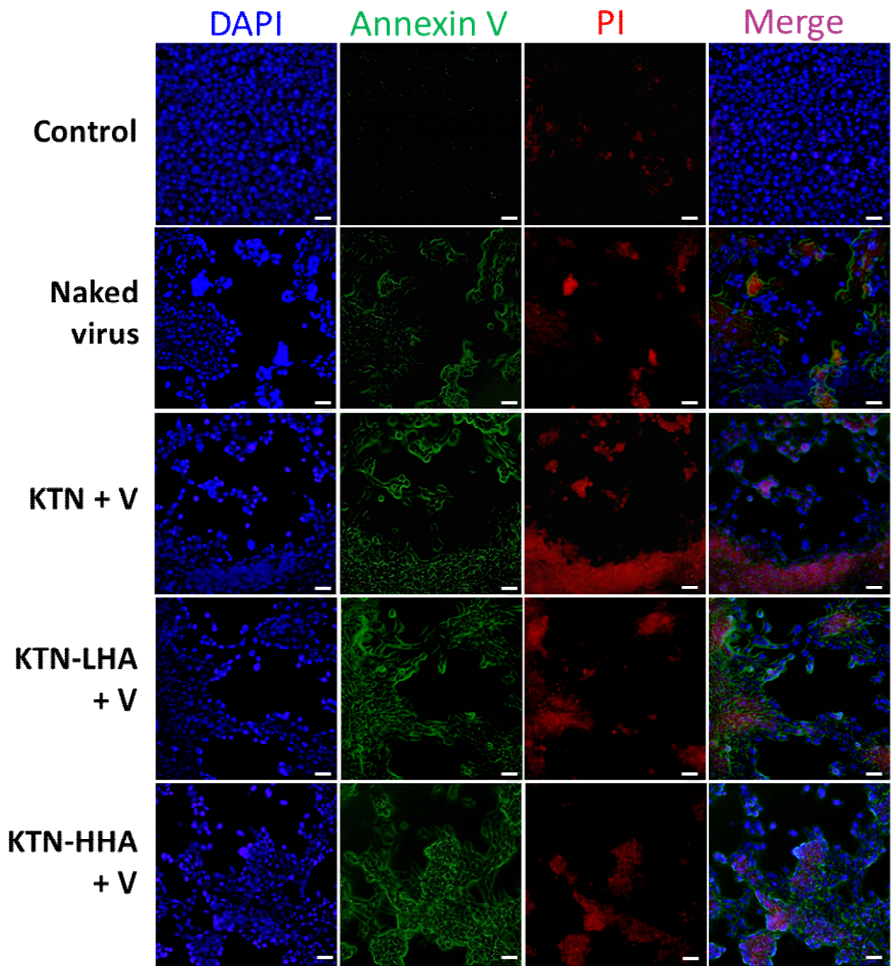

Figure 7. Evaluation of apoptosis imaging by Annexin V/PI staining of KTN-based hydrogels with OVV (MOI 1) in 4T1 mouse breast cancer cell line (Scale bar = 200 μm)

3.6 *In Vivo* Imaging of Hydrogel Localization in Tumor

In order to confirm the residence of KTN-HHA hydrogel in cancer tissues, which had the best anticancer effect in cell experiments, fluorescence Cy5.5 was conjugated and confirmed by imaging (Figure 8) [23-25]. As a result of observation for 14 days after injection of KTN-HHA-Cy5.5 in mouse cancer tissues, it was confirmed that the cancer stays well in both cancer tissues at 6 hours, 1, 2, 6, 8 and 14 days. Fluorescence images are well detected with time, and even if they are loaded with OVV in the hydrogel, they can stay in cancer tissues and expect the release effect.

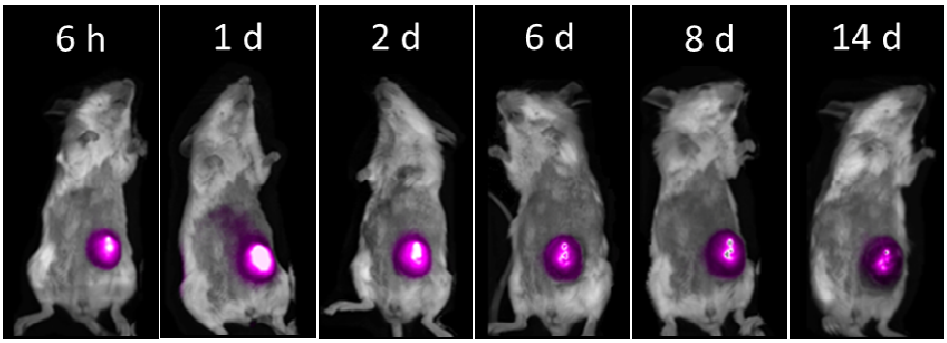

Figure 8. *In vivo* fluorescence images of Cy5.5-labeled KTN-based HA in tumor-bearing BALB/c mouse and stably remained for 14 days

3.7 *In Vivo* Tumor Inhibition Effect

In vivo, the mice were treated with DPBS, Virus, KTN, KTN-HHA, and OVV loaded-KTN and KTN-HHA. We used an orthotopic tumor model by injecting 4T1 mouse breast cancer cells into the right armpit of BALB/c mice. This model made it easier to evaluate the effect on tumor growth and also possible to study the impact of OVV on 4T1 cancer cell population and the antitumoral immune response during the treatments. After treatment of DPBS (Control; CON), empty KTN and KTN-HHA hydrogels, or naked virus (NV), virus loaded KTN (KTN + V) and KTN-HHA (KTN-HHA + V), the tumor volume was measured at the time points, as no significant changes was observed in tumor volume (Figure 9).

The necrotic lesion formation which can be visually confirmed in cancer tissue at the time of autopsy was observed (Figure 10a), and it was confirmed that cancer cell proliferation was most inhibited in the virus administration group although there was a limitation in comparison of the anticancer efficacy in the size (Figure 9) and weight measurement of cancer (Figure 10b).

Histological section of tumor of 4T1 cell bearing mice on day 19 after intratumoral injection of empty or virus loaded KTN-based hydrogels. Hematoxylin and eosin (H&E) staining of tumor sections were shown (Figure 11a). The image was analyzed by microscopy in 20X objective and captured in its entirety using a digital camera. Histological analysis revealed that the proliferation of cancer cells except for necrotic lesions was significantly reduced in all

experimental groups, including KTN and KTN-HHA hydrogels, as compared with the DPBS-treated control group (Figure 11a, b). The necrotic lesion formation which can be visually confirmed in cancer tissue at the time of autopsy was observed, and it was confirmed that cancer cell proliferation was most inhibited in the virus administration group although there was a limitation in comparison of the anticancer efficacy in the size measurement of cancer [26].

Lung metastasis was observed, and metastatic lesion formation was compared with each group (Figure 11c). In all experimental groups, metastatic lesion formation was inhibited compared with control group. The formation of metastatic lesions was least observed in virus-loaded KTN-HHA, confirming the inhibition of metastatic lesions in the order of DPBS, virus, KTN, KTN-HHA, and virus-loaded KTN and KTN-HHA.

In immunohistochemical staining, viruses were observed in the tumor tissues after the administration of the virus (Figure 12). As a result, viruses were not observed in the control group without the virus, but viruses were found in viruses, viruses-loaded KTN and KTN-HHA to remain. In particular, we observed virus infiltration in some tumor proliferative lesions in virus-treated group and virus-loaded KTN. Immunohistochemical staining was performed using antibodies against CD4 and CD8 to identify infiltrating immune cells in tumor tissues. As a result, it was confirmed that the infiltration of the immune cells was increased in both the proliferating tumor and the outer boundary of the tumor. In particular, the increase of CD8 positive cell was observed more prominently than the CD4 positive cell (Figure 12).

Flow cytometry analysis was performed to analyze the correlation between

tumor cell proliferation inhibition and metastatic lesion inhibition and the body's immune response [27, 28] (Figure 13). As a result, it was confirmed that NK cell and cytotoxic T cell were increased compared with the control group. On the other hand, in KTN administration, except for cells expressing Nkp46, all of them were observed to be similar to that of the control group, and the increase of NK cell and cytotoxic T cell was remarkable when the virus was loaded, and the regulatory T cell was not increased compared with the control group, respectively. The increase of MDSC was remarkable when KTN-HHA hydrogel was administered, and other immune cells were similar to those of the control group. On the other hand, when KTN-HHA hydrogel loaded with the virus was administered, it was observed that NK1.1-expressing cells and NK T cells were prominent but cytotoxic T cells and regulatory T cells were not increased.

The antitumor effect of the virus was thought to be due to NK cell and cytotoxic T cell. In the case of administration of KTN or KTN-HHA hydrogel, the increase of the immune cells was limited, while the increase of effector cells such as NK cell, NK T cell, and cytotoxic T cell was observed when the virus was loaded. In addition, the increase of regulatory T cells was prominent at the time of administration of the virus alone, but it was confirmed that no increase of regulatory T cells was observed in the presence of the virus when the KTN or KTN-HHA hydrogel was loaded.

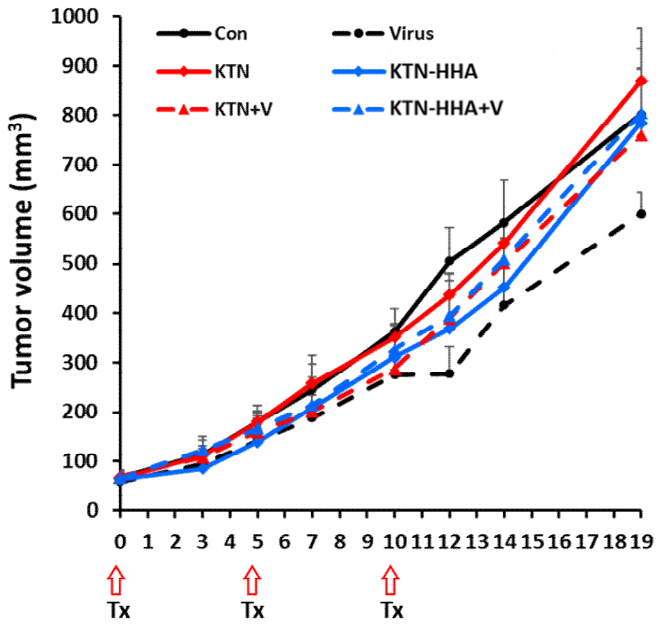

Figure 9. *In vivo* tumor volume growth curve of after treatment of virus loaded KTN-based hydrogels in tumor-bearing BALB/c mouse for 19 days

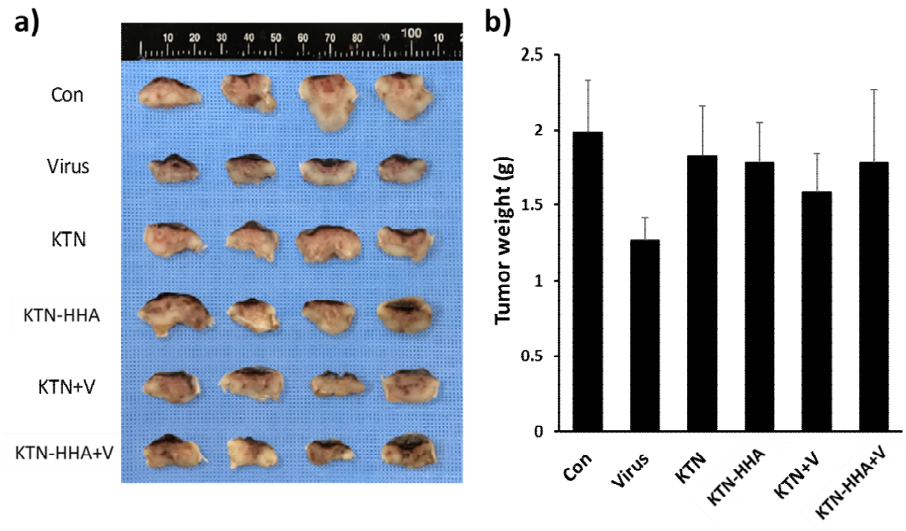

Figure 10. The gross tumor morphology (a) and the terminal tumor weight (b) of 4T1 mouse breast cancer cells bearing mice after intratumoral injection of virus loaded KTN-based hydrogels

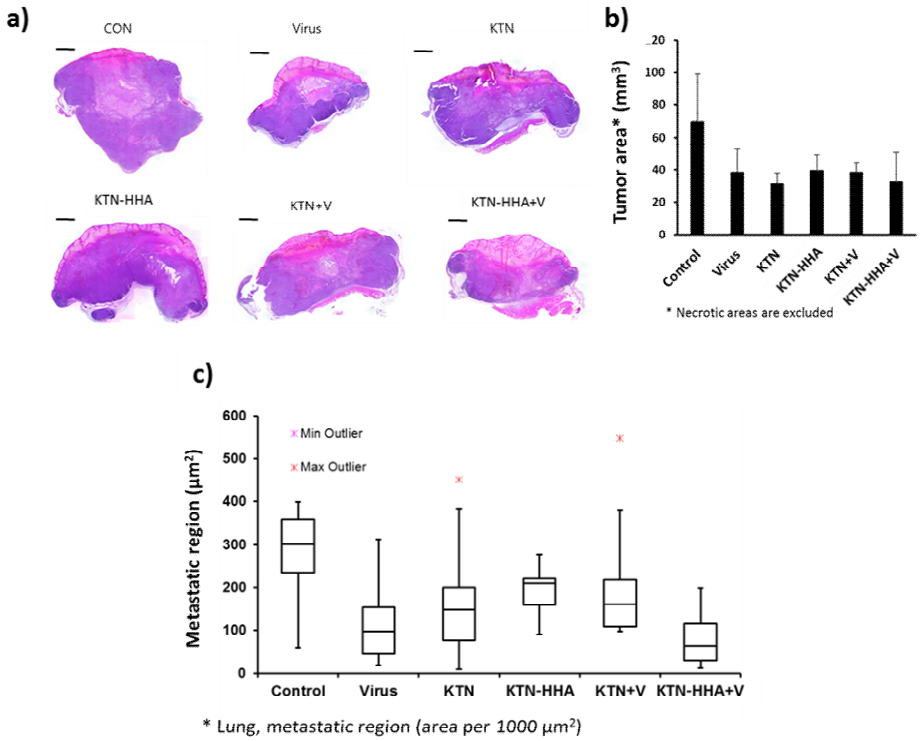

Figure 11. Histological section of tumor of 4T1 cell bearing mice with H&E staining (Scale bar = 2 mm) (a), tumor area analysis excluding tumor necrosis (b), and metastatic region of 4T1 cells on the lung of the mice (c)

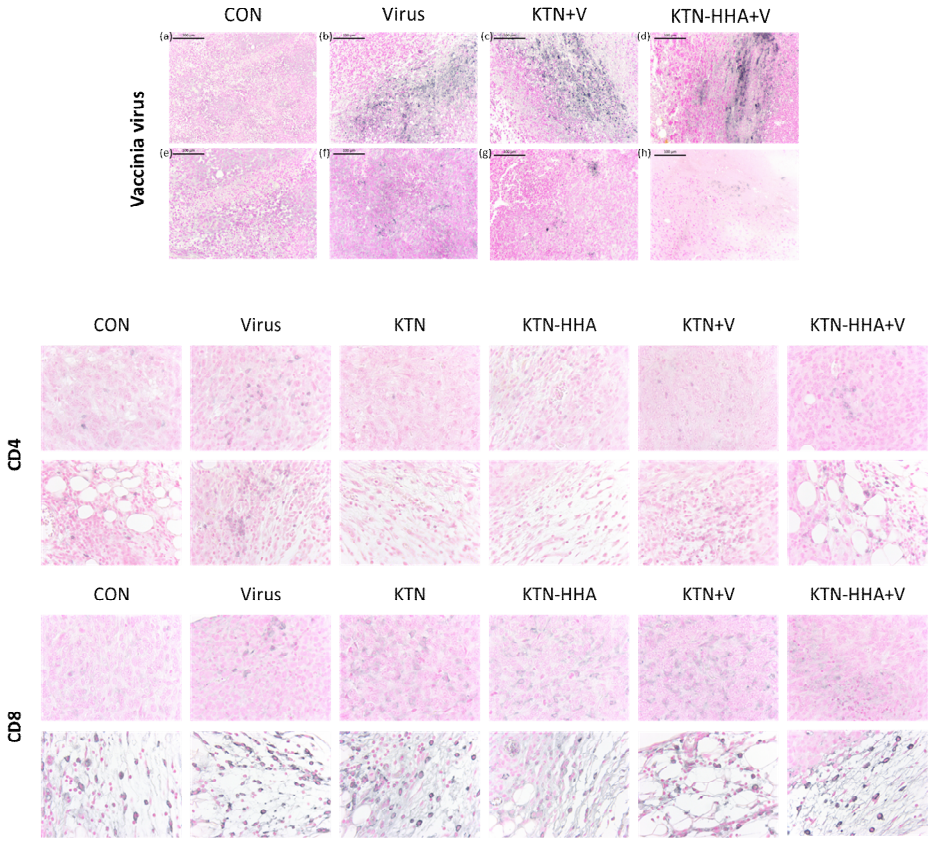

Figure 12. Immunohistochemical staining of virus, CD4 positive cell, and CD8 positive cell infiltration

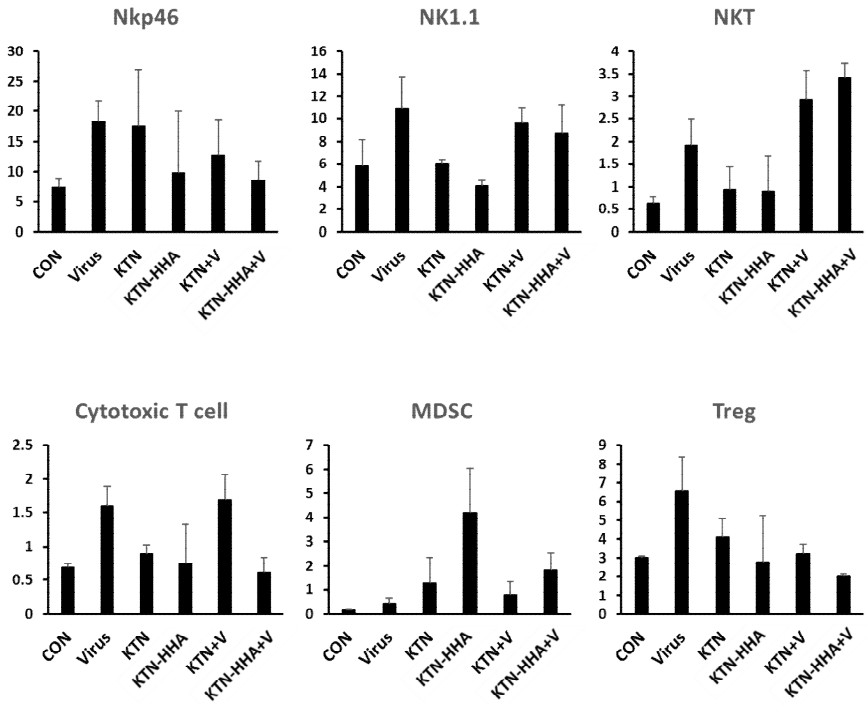

Figure 13. Flow cytometry analysis of immune cell distribution

4. Conclusions

We have developed an injectable hydrogel formulation that can effectively deliver OVV *in vivo* and increase the anticancer effect. The natural protein KTN was extracted from human hair and tested for the possibility of carrier by synthesizing KTN with HA having different molecular weights. The emissive effect of virus from the KTN crosslinked HA hydrogel was found to be greatest through the release test after the OVV was loaded, which is considered to be related to the decrease in the pore size and the increase in the hydrophilic period as shown in the SEM image. In the cell experiments, the anticancer activity was increased as the concentration of virus in the hydrogel was increased, and the anticancer effect was enhanced with KTN. For evaluation of local delivery efficacy with OVV loaded KTN and KTN-HA hydrogels, antitumor evaluation was conducted in animal models of mice of breast cancer. The anticancer activity of OVV can be maximized through the synergistic effect of the anticancer activity of the KTN-based hydrogel as the virus carrier.

5. References

1. Foulkes, W.D., I.E. Smith, and J.S. Reis-Filho, *Triple-negative breast cancer.* New England journal of medicine, 2010. **363**(20): p. 1938-1948.
2. Chacón, R.D. and M.V. Costanzo, *Triple-negative breast cancer.* Breast cancer research, 2010. **12**(2): p. S3.
3. Dent, R., et al., *Triple-negative breast cancer: clinical features and patterns of recurrence.* Clinical cancer research, 2007. **13**(15): p. 4429-4434.
4. Kay, M.A., J.C. Glorioso, and L. Naldini, *Viral vectors for gene therapy: the art of turning infectious agents into vehicles of therapeutics.* Nature medicine, 2001. **7**(1): p. 33-40.
5. Thomas, C.E., A. Ehrhardt, and M.A. Kay, *Progress and problems with the use of viral vectors for gene therapy.* Nature Reviews Genetics, 2003. **4**(5): p. 346-358.
6. Kochneva, G., et al., *Engineering of double recombinant vaccinia virus with enhanced oncolytic potential for solid tumor virotherapy.* Oncotarget, 2016. **7**(45): p. 74171.
7. Kirn, D.H. and S.H. Thorne, *Targeted and armed oncolytic poxviruses: a novel multi-mechanistic therapeutic class for cancer.* Nature Reviews Cancer, 2009. **9**(1): p. 64-71.
8. McCart, J.A., et al., *Systemic cancer therapy with a tumor-selective vaccinia virus mutant lacking thymidine kinase and vaccinia growth fa*

ctor genes. Cancer research, 2001. **61**(24): p. 8751-8757.

9. Stewart, C.J., M. Ito, and S.E. Conrad, *Evidence for transcriptional a nd post-transcriptional control of the cellular thymidine kinase gene.* Molecular and cellular biology, 1987. **7**(3): p. 1156-1163.

10. Nemunaitis, J., et al., *Phase II trial of intratumoral administration of ONYX-015, a replication-selective adenovirus, in patients with refrac tory head and neck cancer.* Journal of Clinical Oncology, 2001. **19** (2): p. 289-298.

11. Sauthoff, H., et al., *Intratumoral spread of wild-type adenovirus is li mited after local injection of human xenograft tumors: virus persists and spreads systemically at late time points.* Human gene therapy, 20 03. **14**(5): p. 425-433.

12. Robbins, P.D. and S.C. Ghivizzani, *Viral vectors for gene therapy.* P harmacology & therapeutics, 1998. **80**(1): p. 35-47.

13. Markowicz, S., et al., *Anticancer properties of peptide fragments of hair proteins.* PloS one, 2014. **9**(6): p. e98073.

14. Dosio, F., et al., *Hyaluronic acid for anticancer drug and nucleic ac id delivery.* Advanced drug delivery reviews, 2016. **97**: p. 204-236.

15. Oh, E.J., et al., *Target specific and long-acting delivery of protein, p eptide, and nucleotide therapeutics using hyaluronic acid derivatives.* Journal of Controlled Release, 2010. **141**(1): p. 2-12.

16. Nimmo, C.M., S.C. Owen, and M.S. Shoichet, *Diels− Alder click cr oss-linked hyaluronic acid hydrogels for tissue engineering.* Biomacro molecules, 2011. **12**(3): p. 824-830.

17. Sierpinski, P., et al., *The use of keratin biomaterials derived from hu man hair for the promotion of rapid regeneration of peripheral nerve s.* Biomaterials, 2008. **29**(1): p. 118-128.

18. Steinert, P.M., *The extraction and characterization of bovine epiderm al α-keratin.* Biochemical Journal, 1975. **149**(1): p. 39-48.

19. Verma, V., et al., *Preparation of scaffolds from human hair proteins for tissue-engineering applications.* Biomedical materials, 2008. **3**(2): p. 025007.

20. Wang, D., et al., *Treatment of metastatic breast cancer by combinati on of chemotherapy and photothermal ablation using doxorubicin-loa ded DNA wrapped gold nanorods.* Biomaterials, 2014. **35**(29): p. 837 4-8384.

21. Ye, M.-X., et al., *Curcumin reverses cis-platin resistance and promot es human lung adenocarcinoma A549/DDP cell apoptosis through HI F-1α and caspase-3 mechanisms.* Phytomedicine, 2012. **19**(8): p. 779-787.

22. Miao, Q., et al., *Anticancer effects of bufalin on human hepatocellula r carcinoma HepG2 cells: roles of apoptosis and autophagy.* Internati onal journal of molecular sciences, 2013. **14**(1): p. 1370-1382.

23. Yang, X., et al., *Mapping Sentinel Lymph Node Metastasis by Dual-p robe Optical Imaging.* Theranostics, 2017. **7**(1): p. 153.

24. Lei, K., et al., *Functional biomedical hydrogels for in vivo imaging.* Journal of Materials Chemistry B, 2016. **4**(48): p. 7793-7812.

25. Luo, W., et al., *Dual-targeted and pH-sensitive Doxorubicin Prodrug-*

Microbubble Complex with Ultrasound for Tumor Treatment. Theranostics, 2017. **7**(2): p. 452.

26. Bastian, A., et al., *A small molecule with anticancer and antimetastatic activities induces rapid mitochondrial-associated necrosis in breast cancer.* Journal of Pharmacology and Experimental Therapeutics, 2015. **353**(2): p. 392-404.

27. Yu, F., et al., *T-cell engager-armed oncolytic vaccinia virus significantly enhances antitumor therapy.* Molecular Therapy, 2014. **22**(1): p. 102-111.

28. Li, J., et al., *Chemokine expression from oncolytic vaccinia virus enhances vaccine therapies of cancer.* Molecular Therapy, 2011. **19**(4): p. 650-657.

요약 (국문초록)

항암 백시니아 바이러스의 국소적 전달을 위한 케라틴 기반 하이드로젤 연구

종양 세포에 직접 작용하여 암을 치료하는 항암 백시니아 바이러스를 효율적으로 생체 내로 운반하고, 항암 효과를 높일 수 있는 국소 투여 하이드로젤 제형에 대한 연구이다. 하이드로젤에 탑재된 항암 백시니아 바이러스는 암 조직의 빽빽한 세포막 사이를 통하여 퍼져나가는 것이 향상되고 암 조직 내 서방출이 가능하여 생체 내 면역 작용에 의한 배출을 최소화시킬 수 있다. 또한 여기서 사용된 사람 머리카락으로부터 추출된 천연 단백질 케라틴은 자체적으로 항암능이 있다고 보고된다. 또한 약물의 서방출이 가능하도록 히알루론산 고분자와 케라틴을 가교시킴으로 친수성의 바이러스가 더욱 하이드로젤 내 오래 머물 수 있도록 하였다. 사람 머리카락에서 추출된 케라틴과 합성된 하이드로젤 모두 특성 분석 및 정상 세포에 대한 독성검사를

통하여 항암 백시니아 바이러스를 운반하기에 유효 물질임을 확인하였다. 바이러스가 탑재된 케라틴과 케라틴-히알루론산 하이드로젤에서의 바이러스 방출평가를 실시함으로 히알루론산의 분자량이 높을 수록 서방출 효과가 높아진다는 것을 확인하였고, 바이러스가 농도별로 다르게 탑재된 하이드로젤의 유방암 세포에 대한 항암 평가도 실시하였다. 세포 실험 결과를 통하여 선별된 케라틴과 고분자 히알루론산이 합성된 케라틴의 항암 백시니아 바이러스 국소 전달 효능 평가를 위하여 실험 쥐 유방암 모델 동물 실험을 진행하였다. 이러한 생체적합적이고 주입가능한 케라틴 기반 하이드로젤을 통하여 항암 백시니아 바이러스의 효율적인 운반의 가능성을 보여주고 있다.

주요어: 항암 바이러스, 주입형 하이드로젤, 국소적 전달, 약물 전달 시스템

학번: 2016-21174